Developing a simple dynamic simulation model of phosphorus in Lake Ontario

Hamid Abdolabadi [a*], Mojtaba Ardestani [b], Amin Sarang [b], John C. Little [c]

[a] *Ph.D Candidate in Environmental Engineering, Graduate Faculty of Environment, University of Tehran.*
[b] *Graduate Faculty of Environment, University of Tehran, Tehran, Iran.*
[c] *Department of Civil and Environmental Engineering, Virginia Tech, Blacksburg, USA.*

*Corresponding Author Tel: +98-915-188-1801; Fax: +98-21-44731988
E-mail address: h.abdolabadi@ut.ac.ir

Abstract
Food cycle creates a mechanism through which nutrients and other components of life are available for living organisms. Improper function of one component of the cycle may lead to emerging disruption in the life cycle of organisms. In this paper, the dynamic behavior of phosphorus was studied by considering three state variables: productive organisms (organic phosphorus), dead organisms (organic phosphorus) and inorganic phosphorus. The system dynamics model intelligibly provides information about changing state variables levels with respect to all interactions and feedbacks. The model was applied to Lake Ontario and run for a year with daily time steps. The model demonstrates acceptable performance in estimating the variables' concentration. Stratification and mixing condition have a significant effect on the variables' concentration during two periods (Day 100 to 158 and day 315 to 335) leading to a decrease in the soluble reactive phosphorus concentration of 80% in the hypolimnion (compared to the epilimnion) as well as an increase of phytoplankton concentration from 0.2 to 0.4 (mg/l) in the epilimnion.
Keywords: Phosphorus cycle, System Dynamics, Phytoplankton, Lake Ontario.

1. Introduction

The food cycle is an ecological process in which nutrients change from one form to another. The existence of the ecosystem depends on this cycle. Without it, productive organisms would not be able to acquire the nutrients necessary for their survival (Föllmi, 1996).

Several processes including solar radiation, prey-predator dynamics, and hydrological and climatic parameters directly affect the food cycle. However, solar energy has the most impact on the natural process of growth and death in nature. The sun supplies the required energy for the plants (producers) and they absorb light to photosynthesize (Deaton & Winebrake, 2000). During photosynthesis, the plants convert light, carbon dioxide, and mineral nutrients to chemical energy so as to produce more complex compounds of carbon, which may then be used as a fuel source for growth. The consumers eat these producers and break down the complex compounds within them to obtain energy and nutrients. After the consumers die, they will be decomposed, and returned to the ecosystem, in the form of a primary nutrient, which can again be used by the producers.

The primary cycle of biomass in the environment is more complex. To simply describe the dynamics of the phosphorus cycle, we should consider at least three storages including the storage of productive organisms (nutrients could be found within them in their living form), dead organisms, and decomposed organisms (bacteria turn the dead organism into primary mineral nutrients) (Föllmi, 1996).

Studying the phosphorus cycle is of paramount significance for assessing water quality. Over the past decades eutrophication has been one of the most common problems affecting water quality of lakes (Andersen et al., 2002; Chapra, 1997; Jong et al., 2002). Eutrophication is a complex natural process occurring gradually due to nutrient enrichment in water bodies which can irreversibly affect the ecosystem. Phosphorous has been recognized as the main limiting factor for algal growth (Gilbert et al., 2010). In most cases, as the concentration of phosphorous declines, the growth rate will also decline due to lack of available nutrients. Therefore, studying the phosphorous cycle in water bodies could be beneficial to clearly understand a simple food web process.

Over the last years, making use of object-oriented models has become very common in analyzing complex phenomena. Such models create a flexible and user-friendly framework to develop up-scaled models for analyzing complex systems (Ahmad & Simonovic, 2000). System dynamics is a feedback based method, which usually does not require advanced mathematical descriptions. Some advantages of such simulation methods are appropriate understanding of a phenomena, high speed numerical calculation, modeling reliability, and the possibility of expanding and easily changing model structure (Loucks et al., 1981; Simonovic & Fahmy, 1999). System dynamics approach has been used for eutrophication models, predicting long-term water quality changes, analysis of the Quality Control policies in river basins, water allocation, and the operation of multi-purpose dams)Mitra & Flynn, 2010; Geene, 1996; Vezjak et al., 1998). In this study, the concentration of phosphorus was simulated with daily time step in three forms i.e. productive organisms (organic phosphorus), dead organisms (organic phosphorus) and inorganic phosphorus. We also used system dynamics to simulate the behavior of phosphorous in lakes during the annual stratification and mixing cycles.

2. Material and Methods

2.1. Model description

The system dynamics approach is a powerful tool for developing object-oriented models to simulate complex phenomena over time that involve feedback effects (Sterman, 2000; Elshorbagy & Ormsbee, 2006). In this study, system dynamics was used to simulate the phosphorus cycle. It is a powerful and simple approach to model complex systems. This approach works based on feedbacks among variables and regulates itself with respect to the past behavior of the system (Forrester, 2007). In these models, an initial causal loop diagram of the desired problem is drawn and a graphical diagram of the model is then plotted using stocks, flows, arrows, and converters (Ford, 1999).

The causal loop diagram of the phosphorus cycle model consists of reinforcing and balancing loops. The combination of positive and negative feedback loops allows the system to reach steady state. Figure 1 shows the causal loop diagrams of the main state variables in the system and their feedback loops.

3. Theory: subsystems of the phosphorus cycle simulation model

As the phytoplankton concentration increases, the concentration of soluble reactive phosphorus will decrease due to consumption. Increasing the phytoplankton concentration leads to greater nutrient uptake. As a result, reducing nutrient concentration slows the growth of phytoplankton (balancing loop). On the other hand, decomposition of phytoplankton increases the concentration of organic compounds. Additionally, if non-soluble phosphorus concentration is on the increase, the nutrient concentration will increase and eventually the phytoplankton concentration will rise (reinforcing loop). All the paramount parameters, their relationships,

and their impacts on the state variables were determined and the structure of the model was developed for each state variable based on its control equations.

In this study, the soluble reactive phosphorus, non-soluble reactive phosphorus and phytoplankton were considered as the key state variables in the epilimnion and hypolimnion. The model was applied to Lake Ontario. To demonstrate the validation and accuracy of the model, we used a range of factors and coefficients suggested by Chapra (1999). This model considers seasonal temperature changes. The stratification divides the lake into two layers (the epilimnion and hypolimnion), which were considered to be completely mixed volumes. Turbulent diffusion connects the two layers and the inputs and outputs flow from the epilimnion. Table 1 defines all symbols used in the following the equations.
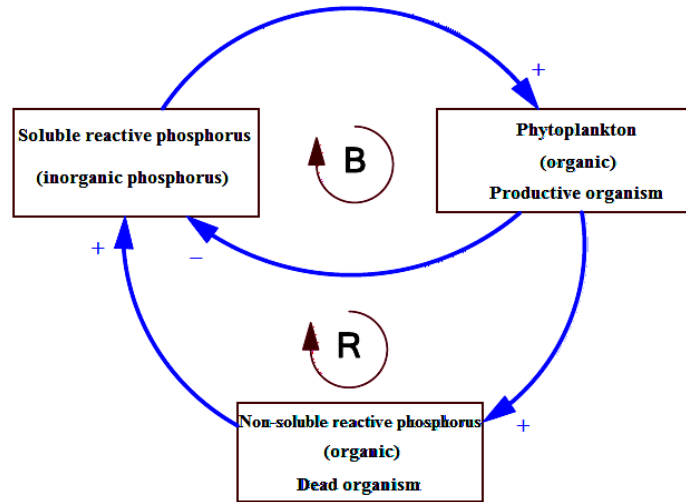

Fig. 1. The causal loop diagram of phosphorus cycle.

Table 1. Values of all the parameters used in the phosphours cycle model

Parameters	Symbol	Value	Parameters	Symbol	Value
Concentration of phytoplankton (mgChla m⁻³)	c_a		Concentration of SRP (mgP m⁻³)	c_{srp}	
Phytoplankton growth rate @ T=20 °C (d⁻¹)	$k_{ga,20}$	2	Thermocline area (m²)	A_t	$185*10^8$
Phytoplankton losses due to respiration and excretion (d⁻¹)	k_{ra}	0.025	Epilimnion volume (m³)	V_e	$254*10^9$
Phytoplankton settling velocity (m d⁻¹)	v_a	0.2	Hypolimnion volume (m³)	V_h	$14*10^{11}$
Optimal light level (ly d⁻¹)	I_s	350	Out flow (m³ yr⁻¹)	Q	$212*10^9$
Temprature factor	θ	1.066	Thermocline diffusion:	v_t	
Attenuation of growth due to light	ϕ_L		Summer-stratified (cm² s⁻¹)		0.13
Attenuation of growth due to phosphorous	ϕ_p		Winter-stratified (cm² s⁻¹)		13
Light extinction due to factors other than phytoplankton (m⁻¹)	k_e'	0.2	Start of summer stratification (d)	t_{sss}	100
Phosphorous half-saturation constant (µgP L⁻¹)	k_{sp}	2	Time of establish stratification (d)	t_{tes}	58
Photoperiod (sunlight fraction of day)	f	Time Series	Onset of end of stratification (d)	t_{oes}	315

Extinction coefficient	k_e		End of stratification (d)	t_{es}	20
Variable load (mg d⁻¹)	W		Epilimnion thickness (m)	H_1	20
Concentration of NSRP (mgP m⁻³)	c_{nsrp}		Hypolimnion thickness (m)	H_2	82
NSRP settling velocity (m d⁻¹)	v_{pn}	0.2	The stoichiometric coefficient for the conversion of phosphorous to phytoplankton (mgP/mg Chl⁻¹)	a_{pa}	1
Decomposition rate for NSRP (d⁻¹)	k_r	0.1			

Equations 1 and 2 are mass balances for the epilimnion and hypolimnion (Chapra, 1997). The subscripts e and h designate epilimnion and hypolimnion for state variables of the phosphorus cycle model.

$$V_e \frac{dc_e}{dt} = W - Qc_e + v_t A_t (c_h - c_e) \pm S_e \tag{1}$$

$$V_h \frac{dc_h}{dt} = v_t A_t (c_e - c_h) \pm S_h \tag{2}$$

3.1. Lake volume
The volumes of the epilimnion and hypolimnion were calculated based on the thermal stratification of the lake. In the model, a state variable was used to simulate the lake volume.

3.2. Phosphorus cycle

3.2.1. Phytoplankton

The growth of phytoplankton is a function of temperature, light, nutrients, and algae. The concentration of algae was represented by the concentration of chlorophyll a (Asmala, 2011; Flynn, 2010).
Equation 3 describes the model of phytoplankton growth. The concentration of phytoplankton in the hypolimnion was calculated based on the settling process from the epilimnion and the effective diffusion between the two layers (Chapra, 1997).

$$V_e \frac{dc_{ae}}{dt} = k_{gae}\left(T, c_{srpe}, I\right) V c_{ae} - k_{rae} V c_{ae} + v_t A_t (c_{ah} - c_{ae}) - v_a A_t c_{ae} \tag{3}$$

$$k_{ga}\left(T, c_{srp}, I\right) = k_{g,20} 1.066^{T-20} \phi_L \phi_P \tag{4}$$

The Michaelis-Menten equation was used to account for nutrient limitations, as follows:

$$\phi_P = \frac{c_{srp}}{k_{sp} + c_{srp}} \tag{5}$$

The following equation considers the effect of light limitation on the phytoplankton growth rate.

$$\phi_L = \frac{2.718 f}{k_e H} \left[exp\left(-\frac{I_a}{I_s} e^{-k_e H_1} \right) - exp\left(-\frac{I_a}{I_s} e^{-k_e H_2} \right) \right] \tag{6}$$

$$k_e = k'_e + 0.0088c_a + 0.054c_a{}^{2/3} \qquad\qquad (7)$$

Figure 2 shows the stock and flow diagram for phytoplankton in phosphorus cycle model.
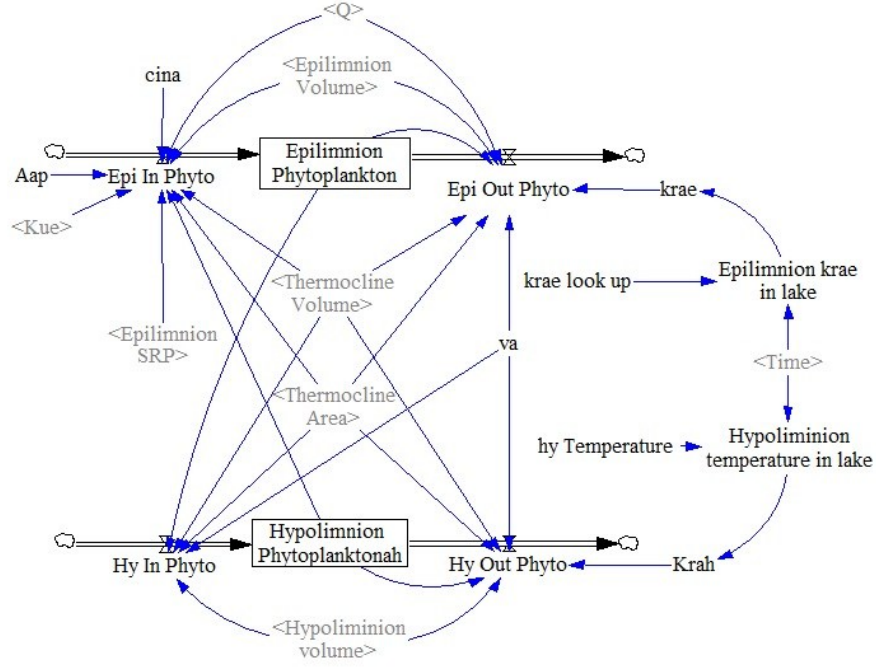

Fig. 2. Stock and flow diagram for phytoplankton.

3.2.3. Non-soluble reactive phosphorous (particulate phosphorus)

Phosphorous is classified into two groups of reactive and non-soluble reactive phosphorous. This classification is due to the method of measuring the phosphorous concentration in the field. In most cases, the phosphorous concentration is measured as reactive soluble phosphorous and total phosphorous. The concentration of non-soluble reactive phosphorous is equal to the difference between these stocks. The particulate phosphorus increases through the decomposition of the phytoplankton, and its concentration is controlled through the decomposition, settling, and decay processes. Eventually, the particulate phosphorus transforms into reactive soluble phosphorous. Equations 9 and 10 describe the non-soluble reactive phosphorous model.

$$V_e \frac{dc_{nsrpe}}{dt} = W_{nsrpe} - QC_{nsrpe} + a_{pa}K_{rae}V_eC_{ae} - K_{re}V_eC_{nsrpe} + \upsilon_t A_t (C_{nsrph} - C_{nsrpe}) - v_p A_t C_{nsrpe} \qquad (9)$$

$$V_h \frac{dC_{nsrph}}{dt} = W_{nsrph} + a_{pa}K_{rah}V_hC_{ah} - K_{rh}V_hC_{nsrph} + \upsilon_t A_t (C_{nsrpe} - C_{nsrph}) + v_p A_t C_{nsrpe} - v_p A_t C_{nsrph} \qquad (10)$$

3.2.3. Soluble reactive phosphorus

Soluble reactive phosphorus is one of the main limiting factors that affect the food chain. Organic phosphorus is converted into soluble reactive phosphorus, which is used by

phytoplankton (Chapra, 1997). Figure 3 shows the stock and flow diagram for soluble and non-soluble reactive phosphorus in the model.

$$V_e \frac{dC_{srpe}}{dt} = W_{srpe} - QC_{srpe} - K_{ge}V_e C_{srpe} + K_{re}V_e C_{nsrpe} + \upsilon_t A_t (C_{srph} - C_{srpe}) \tag{11}$$

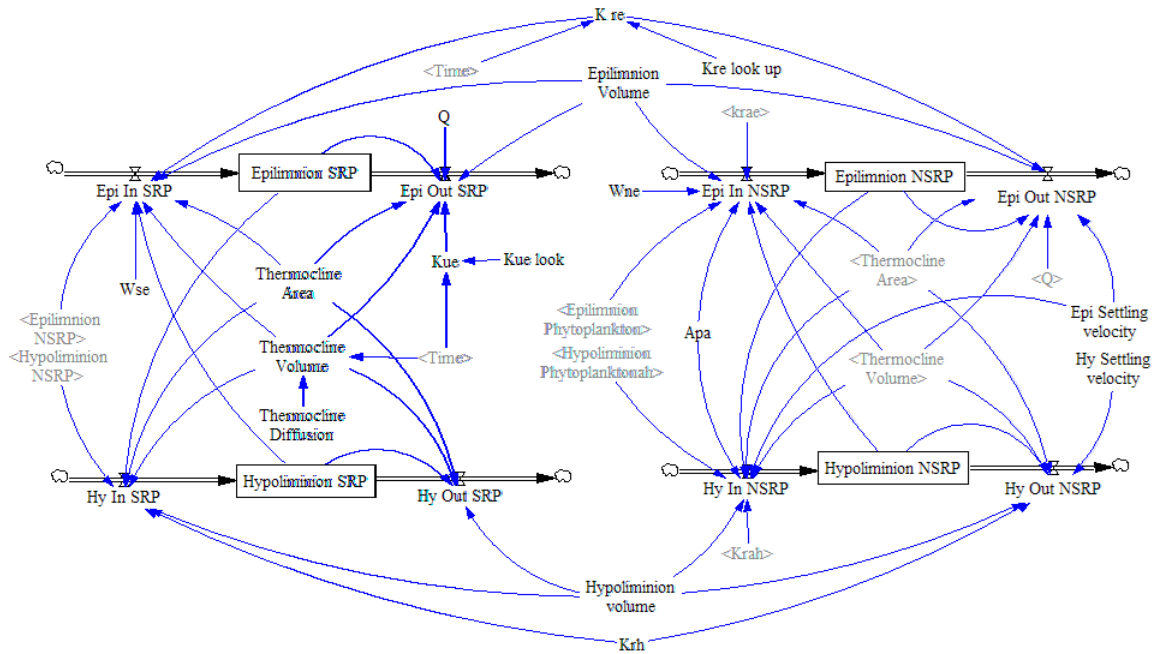$$V_h \frac{dC_{srph}}{dt} = W_{srph} + K_{rh}V_h C_{srph} + \upsilon_t A_t (C_{srpe} - C_{srph}) \tag{12}$$

Fig. 3. Stock and flow diagram for phosphorus.

4. Study site

Lake Ontario is one of the five Great Lakes of North America and it is the 14th largest lake in the world. It is bounded on the north and southwest by the Canadian province of Ontario and on the south by the American state of New York. The Great Lakes watershed is a region of high biodiversity and Lake Ontario is important because of its diversity of birds, fish, reptiles, amphibians, and plants. The lake's primary source is the Niagara River, which drains Lake Erie, while the St Lawrence River serves as the outlet. The drainage basin covers 64,030 km² and 49% of it is forested, 39% is agricultural, while the remaining 13% is urban (Agency USEPA, 1998). The lake has an important freshwater fishery, although it has been negatively affected by water pollution (Christie, 1974). Figure 4 shows Lake Ontario.
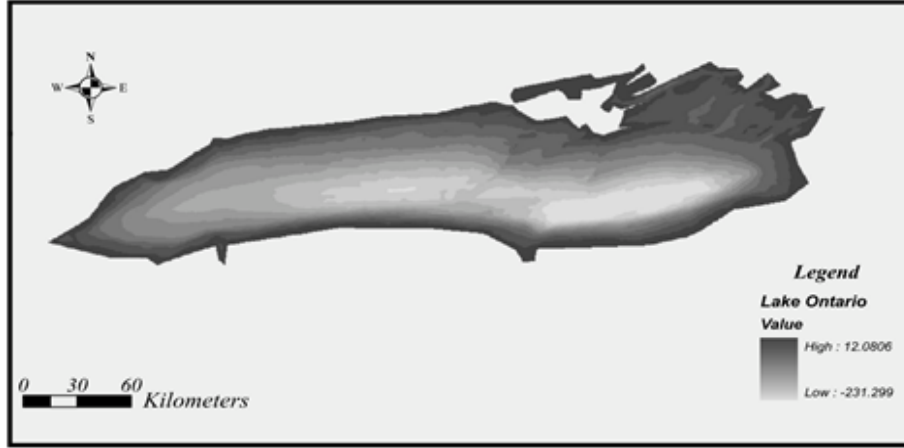
Fig. 4. Lake Ontario.

5. Calibration and validation

To analyze the model behavior and characterize the impact of the parameters on the model's output, a sensitivity analysis of the model was conducted. In this regard, in each model run, the effect of each parameter's changes was quantified, while keeping the other parameters constant. To determine the most important parameters, a relative sensitivity factor was calculated using equation 13 (Shirmohammadi et al., 2006).

$$F_{sa} = \frac{\partial O}{\partial P} \times \frac{P}{O} \qquad\qquad (13)$$

In this equation, "O" is the model's output, and "P" is the model input parameter. The model's parameters were calibrated manually making use of a trial and error method. Table 2 indicates the model's sensitivity analysis for an average concentration of phytoplankton. The sensitivity coefficient reveals that the factors most affecting the lake's phytoplankton concentration were the algae growth rate, phytoplankton decay rate, light extinction, and the decomposition rate of non- soluble reactive phosphorus (NSRP). The range of parameters changes on account of the trial and error, and the closeness of the model's average output and the observed data.

Table 2. The sensitivity coefficient of the phytoplankton concentration in the lake.

Parameters	Symbol	Variation range	F_{sa}
Phytoplankton growth rate	$k_{ga,20}$	0.8 – 1.6	0.623
Phytoplankton losses due to respiration and excretion	k_{ra}	0.02 – 0.04	-0.572
Light extinction due to factors other than phytoplankton	k'_e	0.1 - .0.4	0.532
Decomposition rate for NSRP	k_r	0.05 – 0.2	0.323

After analyzing the sensitivity, the model's error was measured using the Nash-Sutcliff efficiency coefficient, the Pierson correlation coefficient, and the standard error. Nash-Sutcliff efficiency is defined in equation 14:

$$E_{ns} = 1 - \frac{\sum (C_o - C_m)^2}{\sum (C_o - C_{oave})^2}$$ *(14)*

Where C_o is observed variable and C_m is simulated variable. Nash–Sutcliffe efficiencies can range from $-\infty$ to 1. An efficiency of 1 (E = 1) corresponds to a perfect match of estimated outcomes to the observed data. An efficiency of 0 (E = 0) indicates that the model predictions are as precise as the mean of the observed data (Nash & Sutcliff, 1970). According to Table 3 the appropriate accordance of the model's output with the observed data is indicated by a value of the Nash-Sutcliff coefficient (E_{ns}) close to 1, the data correlation coefficient (R), and also a low standard error for the model's calibration and verification periods. The result indicates a reliable model definition. Figure 5 shows observed data and simulation results for soluble reactive phosphorus in the epilimnion and hypolimnion of Lake Ontario. It can be seen that the correlation between estimated and observed data for phosphorus is very close in both layers.

Table 3. The results of Nash-Sutcliff coefficient, correlation coefficient, and the standard error.

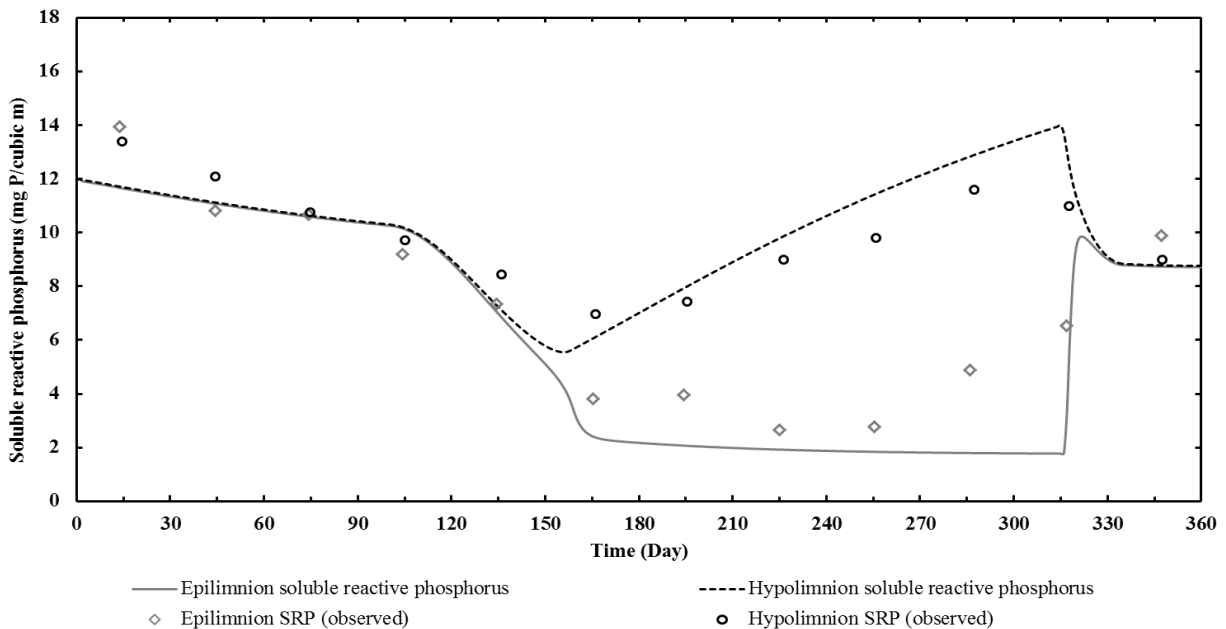| Layer / Criterion	r	S_e	E_{ns}
Epilimnion	*0.966*	*1.5*	*0.84*
Hypolimnion	*0.86*	*1.07*	*0.68*

Fig. 5. The observed and simulated concentrations of the soluble reactive phosphorus.

Specific tests can be utilized to assess the accuracy of a model, based on the system dynamics approach, as described below.

5.1. The dimensional analysis test
The unit consistency of each state variable in the model was analyzed by the Units Check order. If there is an inconsistency in units, a unit error will emerge. Although a dimensional error does

not affect the numerical calculation and the model's outcomes, it can lead to misunderstanding for complex systems. In this study, there is no unit error in the model.

5.2. Extreme conditions test
Every model must cope with extreme circumstances during the simulation period. For this reason, the input load and initial concentration of SRP, NSRP, and phytoplankton load were considered as 0. Accordingly, the phytoplankton concentration decreases from the initial amount of 1 to 0.4 mg Chla per cubic meter (Figure 6). In addition, the SRP and NSRP concentrations increase during the simulation owing to decomposition of the phytoplankton. Consequently, the model works accurately under extreme conditions.
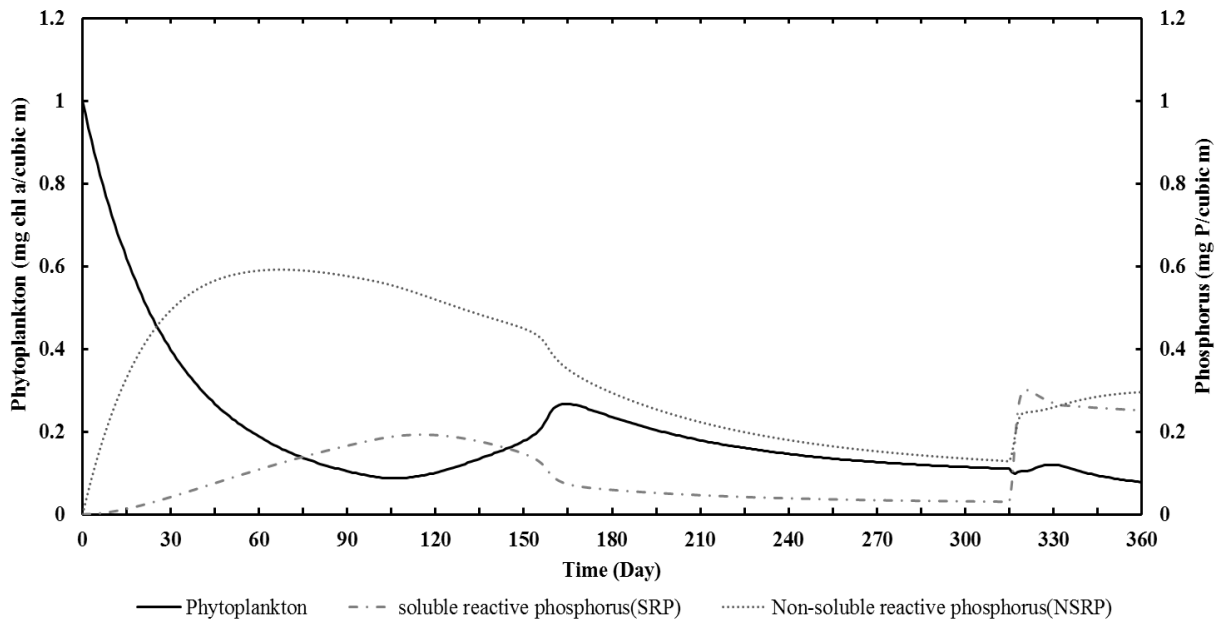

Fig 6. The results of state variable concentration under extreme Conditions.

6. Results and Discussion
After developing the model structure for the epilimnion and hypolimnion of the lake based on their equations, the concentration of soluble reactive phosphorous, non-soluble reactive phosphorous, total phosphorous, and algae (phytoplankton) stocks were analyzed from January to December. To assess the simulation results, we first analyze the behavior of the state variables separately for each layer. Figure 7, shows the simulation results in the epilimnion.
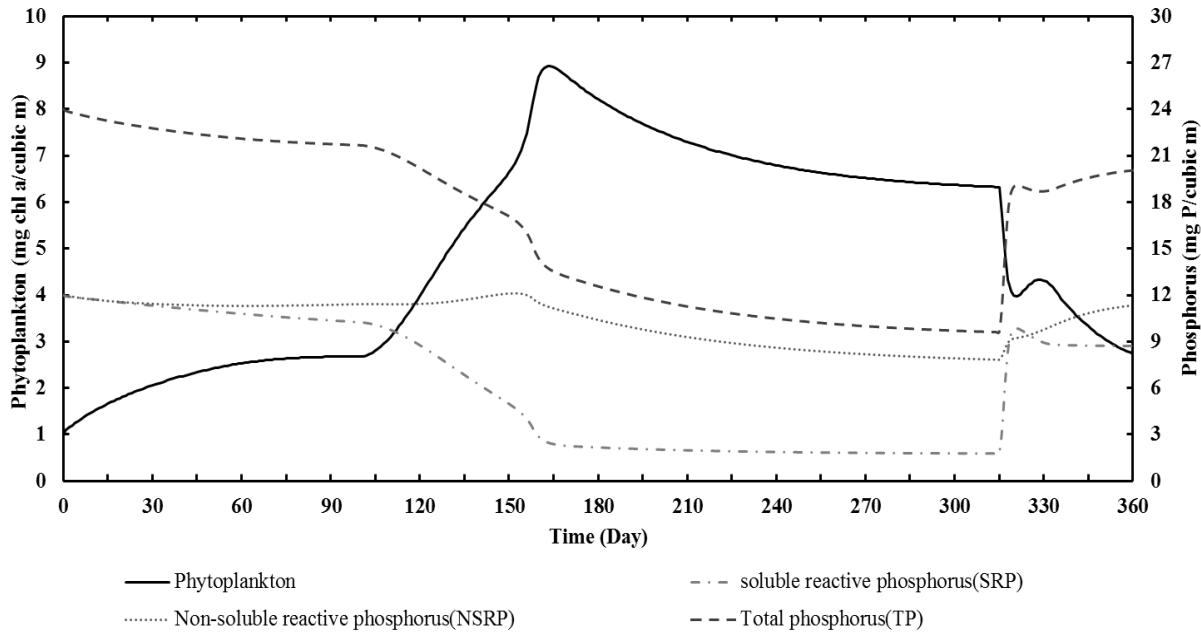
Fig 7. Simulation results for state variables in the epilimnion.

According to Fig. 7, the phytoplankton growth rate increases slightly during the first two months of the year. This might be due to the gradual increase in light and the photoperiodic ratio. These factors approximately neutralize and control the growth of phytoplankton.

The phytoplankton concentration increases abruptly due to the abundance of soluble reactive phosphorous and a dramatic rise in temperature and solar radiation. The phytoplankton concentration reaches a peak on about Day 160 when the summer stratification develops, and afterwards, until the end of the thermal stratification, has a gradual decreasing trend. As pointed out in the modeling section, the phytoplankton decay rate parameter (K_r), which includes respiration, decomposition and excretion processes, is the most important factor controlling the phytoplankton concentration. This parameter increases when the temperature increases based on the Michael-Manten equation. Therefore, the reason for the gradual decrease in the phytoplankton concentration during the summer could be due to the increase of this parameter. Eventually, the interaction of both feedback loops could be recognized as the main reason for the maximum phytoplankton concentration at 9 (mg Chla/cubic m) on about Day 160. The soluble reactive phosphorous is a primary nutrient for algae growth. Its concentration declines rapidly as the algae begins to grow. It reaches the minimum concentration of 2 (mg P/cubic m) on about Day 160 when the phytoplankton concentration peaks. The trade-off between phytoplankton growth and death causes SRP to gradually reduce in the epilimnion throughout the summer up to about Day 315.

Since the level of non-soluble reactive phosphorous increases with phytoplankton decay, its concentration increases slowly because of the slow growth of algae and the continued entry of input loads. After Day 160, the non-soluble reactive phosphorous concentration decreases in the epilimnion, alongside the reduction in the phytoplankton concentration, and slowly continues through Day 315.

Strong vertical mixing occurs during the late summer when the phytoplankton concentration declines and the SRP and NSRP concentrations increase. Figure 8, shows the simulation results for state variables in the hypolimnion.
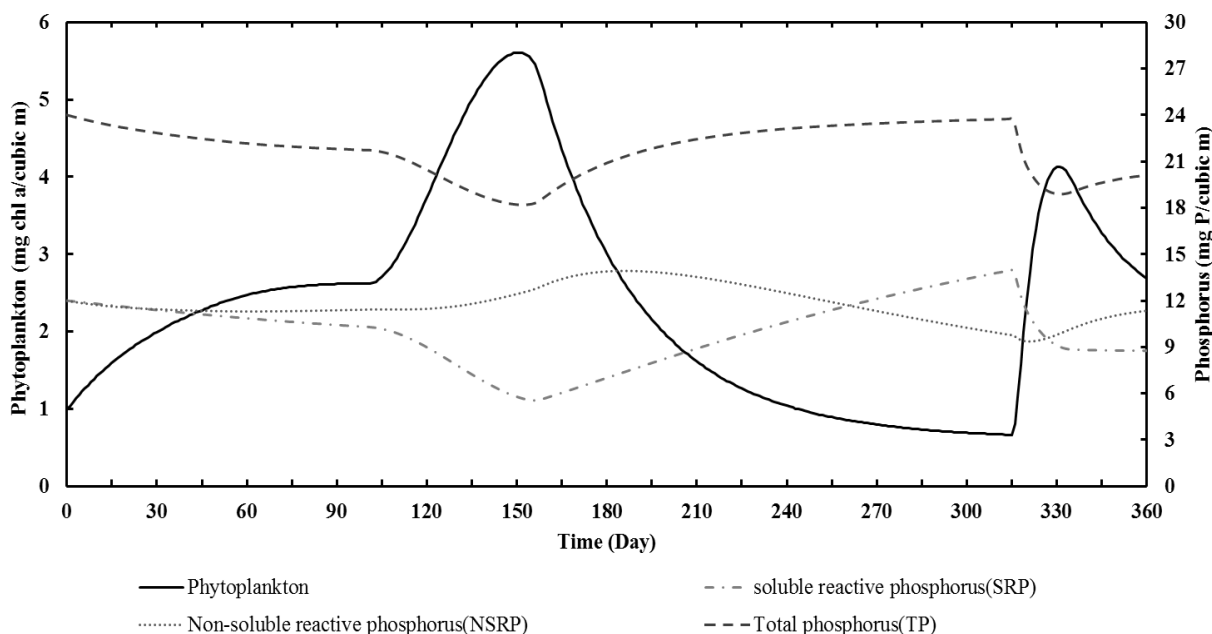
Fig 8. The results of phosphorus simulation in the hypolimnion.

The phytoplankton concentration reaches a maximum of 5.5 (mg Chla/cubic m) on about day 150 in the hypolimnion, and after that, its concentration significantly decreases because of light limitation (caused by the algal bloom in the epilimnion) and decomposition and excretion processes. During the summer stratification, temperature remains almost unchanged in this layer. As a result, the phytoplankton concentration in the hypolimnion is smaller than in the epilimnion. Soluble reactive phosphorous increases in the hypolimnion due to the reduction of phosphorous consumption, the settling of algae and non-soluble reactive phosphorous from the epilimnion, and the decomposition process. The other important point is the fluctuation in the phosphorous concentration in the epilimnion and hypolimnion on Day 315. As the water is getting cold in the upper layer in the late summer, it will be denser which causes destratification of the lake.

The non-soluble reactive phosphorous concentration in the hypolimnion is higher than the epilimnion owing to settling of the non-soluble reactive phosphorous from the epilimnion, and phytoplankton decay in the hypolimnion. The non-soluble reactive phosphorous concentration gradually decreases during the stratification period based upon the reduction in phytoplankton concentration, and eventually on Day 315 it equals the non-soluble reactive phosphorous concentration in the epilimnion at around 9 (mg P/cubic m).

The total phosphorous concentration in the epilimnion (accumulation of the soluble and non-soluble reactive phosphorous) decreases during the thermal stratification period due to the phytoplankton consumption (Fig. 7). Moreover, it declines in the hypolimnion in two time periods (Fig. 8). The first of these is the time of establishing stratification in the lake between Day 100 and Day158, and the second period is the time of turning over between Day 315 and Day335.

7. Conclusion

In this study, the phosphorous cycle in a lake was simulated using a system dynamics approach. The results show that the model has the capability to simulate the behavior of the phosphorous cycle. In this model, the overall trends and fluctuations of the phytoplankton (productive organisms), non-soluble reactive phosphorus (dead organisms), and soluble reactive phosphorus (inorganic phosphorous) were studied. Despite the similar overall behavior of the variables in the upper and lower layer, the results revealed that the peak concentration of the phytoplankton was smaller in the hypolimnion. It was also shown that the concentration of state variables were affected by the stratification and the complete mixing condition.

The model could be used to demonstrate the interactions and feedbacks of components of the phosphorous cycle. It also can provide students, decision-makers and operators with an interactive learning environment to evaluate the effectiveness of management policies. Finally, adding a more comprehensive carbon cycle and including the release of phosphorous from the sediments would improve the model reliability, although this will increase the model complexity and the need for more accurate data.

References

Ahmad, S., Simonovic, S.P., 2000. Dynamic modeling of flood management policies. In Proceedings of the 18th International Conference of The System Dynamics Society: Sustainability in the Third Millennium, Bergen, Norway, 6-10.

Anderson, D.M., Glibert, P.M., Burkholder, J.M., 2002. Harmful algal blooms and eutrophication: nutrient sources, composition, and consequences. Estuaries 25, 704–726.

Asmala, E., Saikku, L., Vienonen, S., 2011. Import–export balance of nitrogen and phosphorus in food, fodder and fertilizers in the Baltic Sea drainage area. Science of the Total Environment 409(23), 4917-4922.

Chapra, S.D., 1997. Surface water quality modeling. 1th Edition, Mc Graw-Hill, Inc.

Deaton, M. L., Winebrake, J. J., 2000. Dynamic modeling of environmental systems, Springer Verlag.

Elshorbagy, A., Ormsbee, L., 2006. Object-oriented modeling approach to surface water quality management. Environmental Modeling Software 21(5), 689–698.

Flynn, K.J., 2010. Ecological modelling in a sea of variable stoichiometry; dysfunctionality and the legacy of Redfield and Monod. Progress in Oceanography 84, 52–65.

Föllmi, K., 1996. The phosphorus cycle, phosphogenesis and marine phosphate-rich deposits. Earth-Science Reviews, 40(1): 55-124.

Ford, A., 1999. Modeling the environment: an introduction to system dynamics modeling of environmental systems, Island press.

Forrester, J.W., 2007. System dynamics a personal view of the first fifty years. System Dynamics Review 23(2-3), 345-358.

Geene, B., 1996. Eutrophication of Droodzen reservoir in Iran. Disseratition for the degree of doctor of science (tecnology), Wageningen.

Glibert, P.M., Allen, J.I., Bouwman, L., Brown, C., Flynn, K.J., Lewitus, A. and Madden, C. 2010. Modeling of HABs and eutrophication: status, advances, challenges. Journal of Marine Systems, 83, 262-275.

Jonge, V. N. de, Elliott, M. , Orive, E., 2002. Causes, historical development, effects and future challenges of a common environmental problem: eutrophication. Hydrobiologia 475/476, 1–19.

Loucks, D. P., Stedinger, J.R., Haith, D.A., 1981. Water resources systems planning and analysis. 1th Ed., Prentice Hall, Englewood Cliffs, New York.

Mitra, A., Flynn, K.J., 2010. Modelling mixotrophy in harmful algal blooms: More or less the sum of the parts? Journal of Marine Systems 83, 158-169.

Shirmohammadi, A., Chaubey, I., Harmel, R. D., Bosch, D. D., Muñoz-Carpena, R., Sexton, A., Arabi, M., Wolfe, M. L., Frankenberger, J., 2006. Uncertainty in TMDL models, Transactions of the ASAE 49(4), 1033-1049.

Simonovic, S.P., Fahmy, H., 1999. A new modeling approach for water resources policy analysis. Water Resources Research 35 (1), 295-304.

Sterman, J. D., 2000. Business dynamics; system thinking and modeling for a complex world. Irwin McGraw-Hill Publication.

Vezjak. M., Savsek. T., Stuhler. E. A., 1998. System dynamics of eutrophication process in Lakes. European Journal of Operational Research 109, 442-451.